

## Double-Spin-Flip Resonance of Rhodium Nuclei at Positive and Negative Spin Temperatures

J. T. Tuoriniemi, T. A. Knuuttila, K. Lefmann,\* K. K. Nummila,† and W. Yao‡

*Low Temperature Laboratory, Helsinki University of Technology, P.O. Box 2200, FIN-02015 HUT, Finland*

F. B. Rasmussen

*Niels Bohr Institute, University of Copenhagen, Universitetsparken 5, 2100 København Ø, Denmark*

(Received 20 July 1999)

Sensitive SQUID-NMR measurements were used to study the mutual interactions in the highly polarized nuclear-spin system of rhodium metal. The dipolar coupling gives rise to a weak double-spin-flip resonance. The observed frequency shifts allow deducing separately the dipolarlike contribution and the isotropic exchange term. For the first time, such measurements were extended to negative absolute temperatures as well. We find an effective dipolar moment  $0.10\mu_N$  of which about 15% is attributed to a conduction electron mediated pseudodipolar interaction. The isotropic exchange is described by  $R = -0.9 \pm 0.1$ .

PACS numbers: 76.60.-k, 75.50.Ee

Spontaneous magnetic ordering of nuclear spins in various materials has been made possible by the development of cooling techniques at the microkelvin regime and below [1]. Such investigations are motivated by the fact that interactions between the nuclear spins are often fairly simple and theoretical predictions can be made from first principles. In metals the relevant processes are the dipolar interaction and the conduction-electron mediated indirect-exchange interaction.

NMR measurements at low magnetic fields, comparable with the internal fields arising from the nuclear magnetic moments, can yield direct information about the mutual coupling of the spins. In particular, the dipolar interaction between the nuclei allows a single photon to flip two or more spins, giving rise to resonances at integer multiples (harmonics) of the Larmor frequency. Additionally, weak resonances appear in the parallel-field geometry, where the NMR excitation field is applied along the static magnetic field. The existence of these modes has been theoretically predicted rather early [2,3]. The first experimental demonstration was made indirectly by Anderson [4], and later Kohl *et al.* were able to observe up to four-spin-flip resonance of hydrogen nuclei by employing SQUID NMR [5]. A study of copper metal [6], where the strength of the indirect-exchange interaction was determined by observing a frequency shift of the double-spin-flip resonance at high nuclear polarization, deserves special attention. More recently, Moyland *et al.* investigated theoretically the behavior of the double-spin-flip mode in the noble metals silver and gold [7] that are suitable for studies of nuclear magnetic ordering [1,8,9].

In the present paper we report the observation of the double-spin-flip resonance of nuclei in rhodium metal. For the first time, the phenomenon was observed at a negative spin polarization as well. To analyze the behavior quantitatively we apply a model including a dipolar term and an isotropic exchange interaction according to the guidelines of Refs. [6] and [7]. The essential observables are the

frequency of the primary Larmor mode and of the second harmonic, which are slightly shifted from the exact Larmor and double-Larmor positions. Fortunately, the resonance frequency is a quantity that can be determined with good accuracy even for relatively weak signals. The contributions of the dipolar term and of the exchange term can be separated, since the latter does not shift the main line, but does influence the double-spin resonance.

To achieve sufficiently high nuclear polarization of rhodium (spin  $I = \frac{1}{2}$ , magnetic moment  $\mu = -0.088\mu_N$ ) we employed a cascade nuclear demagnetization cryostat [10]. A massive copper-nuclear stage served as a thermal reservoir below  $100 \mu\text{K}$  for a period of several days. The sample was polarized in a magnetic field of 7 T for about 60 h during which the spin-lattice relaxation (Korringa constant  $\kappa = 8.1 \text{ s K}$  [11]) brought the spin system close to thermal equilibrium with the lattice at  $100\text{--}200 \mu\text{K}$ . Subsequently, the sample was adiabatically demagnetized to the measuring field below 1 mT. The maximum nuclear polarization was  $p = 0.86$  corresponding to a spin temperature of about 250 pK in zero magnetic field. Negative spin polarization was produced by a rapid reversal of the magnetic field (typically at  $400 \mu\text{T}$ ) [12,13]. The best value so achieved was  $p = -0.49$ .

The sample (nominal purity 99.99%) was a slab-shaped single crystal with dimensions  $0.4 \times 5 \times 25 \text{ mm}^3$ . The polarizing field, as well as the NMR pickup coil, were parallel to the longest dimension. The static NMR field was typically along the second longest axis. The demagnetization field within such a sample is approximately that of an ellipsoid with corresponding primary axes. Our dimensions yield demagnetization factors 0.91, 0.08, and 0.01 accordingly [14]. For this crystal, the skin depth was equal to the thickness of the sample at about 100 Hz. The eddy-current screening resulted in the poor flipping efficiency for producing negative polarizations.

The response of the spin system was measured by continuous wave NMR utilizing a dc SQUID. Good signal to

noise ratio was achieved by using a planar second-order gradiometric pickup coil. The excitation amplitude was typically less than 5 nT in order not to deplete the nuclear polarization during the sweep through the resonance. The measuring circuitry had a bandwidth from about 10 Hz to 1 kHz. The nuclear polarization was deduced from the area of the Larmor resonance at  $f = 431$  Hz. The polarization scale was fixed at relatively high temperatures between 0.3 to 1.5 mK against a Pt NMR thermometer on the copper nuclear stage.

The existence of the double-spin-flip mode at about twice the Larmor frequency is perhaps best demonstrated when the excitation field is parallel with the static field. The two peaks have comparable intensity, since also the primary resonance is then given rise to by the dipolar coupling of the spins [3,4]. The absorption peaks in Fig. 1 have been deduced from the decay rate of a low-frequency susceptibility signal during a frequency sweep of an ac excitation modulating the static field. The low-frequency signal (the inset of Fig. 1), driven by 160 nT at 8 Hz perpendicular to the static field, is essentially proportional to the nuclear polarization. The ac modulation amplitude,  $2.5 \mu\text{T}$ , along the static field was adjusted so that it causes a notable decrease of polarization at the absorption maxima. The frequency sweep from 650 to 150 Hz was made in 90 min. Absorption in arbitrary units was calculated as  $(d\chi_{8\text{ Hz}}/dt)/\chi_{8\text{ Hz}}$ .

The double-excitation method of detection described above has the advantage that it is sensitive exclusively to the absorption part, so that no dispersion signal is mixed in by erroneous adjustment of the phase. Also, the baseline is essentially zero, which allows unbiased determination of the shape of the double-spin resonance. The behavior in the tails provides conclusive evidence to dis-

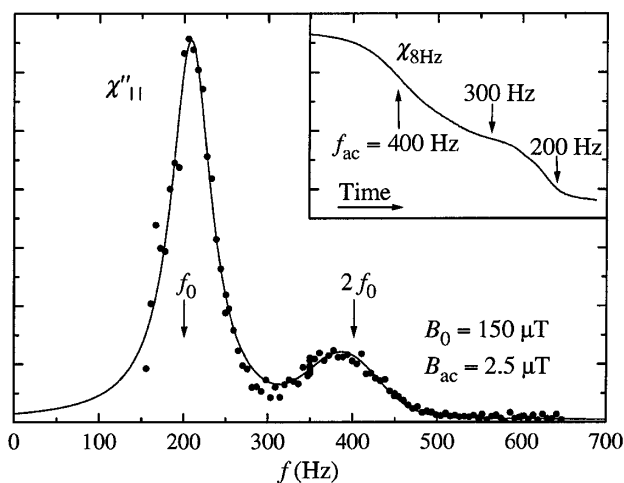


FIG. 1. Parallel field absorption in  $150 \mu\text{T}$  measured by a double-excitation method (see the text). Inset: Low-frequency susceptibility signal during a frequency sweep. The decay of the signal was used to determine the longitudinal absorption as a function of the excitation frequency.

tinguish between Lorentzian or Gaussian shapes. The resolution of our measurements was good enough to conclude that the main peak is very close to Lorentzian in shape, whereas the double-spin resonance is Gaussian. On theoretical grounds, it has been argued that the main resonance should approach a Lorentzian shape at high nuclear polarization [15]. Further, the observations are perfectly understandable on the basis of an analysis of the moments of the harmonic lines within a model including the dipolar and isotropic exchange terms [3].

The absorption peaks in the parallel-field measurement of Fig. 1 are shifted slightly from the exact Larmor and double-Larmor frequencies,  $f_0$  and  $2f_0$ . However, a quantitative analysis of the shifts will be made for the ordinary orthogonal-field geometry only. The static field was swept at a constant excitation frequency to avoid the need for further corrections to the data due to varying skin depth. An example of the data is shown in Fig. 2. The excitation field was 50 nT at 391 Hz, while the orthogonal static field was swept from  $550 \mu\text{T}$  to zero in 8 min. The phase has been adjusted so that the signal separates approximately to the absorption and dispersion parts. In such measurements, the double-spin-flip mode was resolvable in the frequency range from 131 to 831 Hz. At lower frequencies it became indistinguishable from the main line, whereas at higher frequencies it became too weak, as its intensity is proportional to  $1/f^2$ .

According to the theory, the resonances occur at frequencies [6,7]

$$\begin{cases} f_1 = f_0 + \frac{1}{2}(1 - 3D)f_s p, \\ f_2 = 2f_0 + 2(R + \frac{1}{3} - D)f_s p, \end{cases} \quad (1)$$

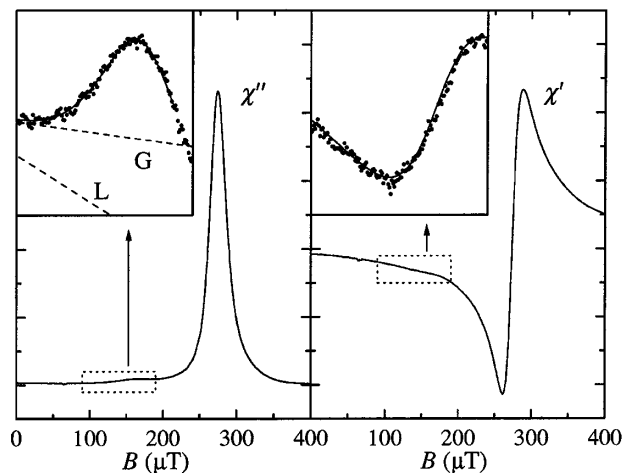


FIG. 2. Larmor resonance and the double-spin-flip satellite at  $f = 391$  Hz and  $p = 0.57$ . Absorption and dispersion are shown in the left and the right frame, respectively. The insets show closeups of the second harmonic, where a Lorentzian fit for the main line has been subtracted. Lines marked by  $G$  and  $L$  show the required baseline if the double-spin-flip absorption is fitted by a Gaussian or Lorentzian line, respectively.

where  $f_0 = \mu B/Ih$  is the Larmor frequency,  $D$  is the demagnetization factor along the static field, and  $R$  is the relative exchange parameter,  $R = \sum_j J_{ij} I/hf_s$ . The ‘‘dipolar frequency’’ is  $f_s = \mu_0 \mu^2 \rho/Ih + f_{pd}$ , where a small pseudodipolar contribution  $f_{pd}$  has to be included in order to explain the observations on rhodium [16,17]. Here,  $\rho$  is the atom number density. Because of the polarization dependent frequency shifts in Eq. (1), the two modes appear to cross at a nonzero field value

$$B_{\times} = -(2R + \frac{1}{6} - \frac{1}{2}D)Ihf_s p/\mu. \quad (2)$$

With  $p > 0$  (and  $D < 1/3$ ), the crossing occurs at a finite applied magnetic field, when the exchange interaction is antiferromagnetic ( $R < 0$ ), as in rhodium [18]. Close to the crossing field, the coupling of the two modes with each other becomes relevant, producing repulsion of the lines. The resonance frequencies given by the coupled equations of motion for the single spins and for the pairs of spins are [6,7]

$$f_{\pm} = \frac{1}{2}(f_1 + f_2 \pm \sqrt{(f_1 - f_2)^2 + 4A}), \quad (3)$$

where the parameter  $A$  describes the strength of the coupling. It results from the terms in the Hamiltonian that do not commute with the single-spin-flip operator  $I^+$ . Deviation from (1) is expected when  $f_1 - f_2 \lesssim 2\sqrt{A}$ , which, however, could not be resolved from our data by just examining the resonance frequencies.

The measured resonance fields  $B_1$  and  $B_2$  immediately give the crossing field as  $B_{\times} = 2B_2 - B_1$ . The relationship (2) is demonstrated in the inset of Fig. 3, where measurements at the full range of frequencies with varying  $p$

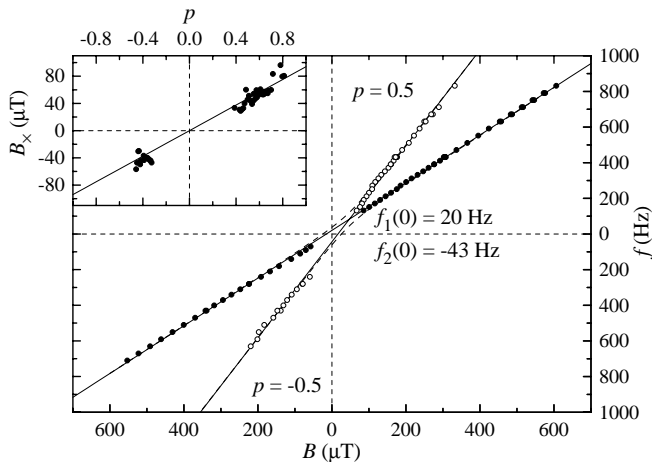


FIG. 3. Resonance frequency versus magnetic field of the Larmor and double-spin-flip modes. The data are reduced to  $|p| = 0.50$ . The data fall on two straight lines with the slopes  $\mu/Ih$  and  $2\mu/Ih$  (solid lines). The shifts from the origin,  $f_1(0)$  and  $f_2(0)$ , result from the dipolar and indirect exchange interactions between the spins. The dashed lines represent a model with coupled equations of spin motion, Eq. (3). The inset: Polarization dependence of the line crossing field  $B_{\times}$  of the two resonances as deduced from the individual spectra at various frequencies.

have been collected. The negative  $B_{\times}$  for negative nuclear polarization indicates that the two peaks have shifted farther apart from each other and no crossing occurs at realizable magnetic fields. The slope of the linear fit gives the quantity  $-(2R + \frac{1}{6} - \frac{1}{2}D)Ihf_s/\mu = 94 \pm 4 \mu\text{T}$ . The contributions of the two parameters of interest,  $R$  and  $f_s$ , can be separated as shown in the following.

A resonance field versus excitation frequency plot at a given nuclear polarization can be compiled by correcting for the  $p$  dependence of the data by means of Eq. (1). The data, reduced to  $|p| = 0.5$ , is shown in Fig. 3. Linear fits to the Larmor and double-spin resonance frequencies with slopes  $\mu/Ih$  and  $2\mu/Ih$ , respectively, indicate offsets  $f_1(0) = 20 \pm 1 \text{ Hz}$  and  $f_2(0) = -43 \pm 2 \text{ Hz}$  at  $B = 0$ . The resonance frequency of the main line is affected to some extent by the eddy currents induced in the sample. Their contribution amounts up to a few Hz at intermediate frequencies and is too small to cause any notable nonlinearity in Fig. 3. The double-spin resonance, on the other hand, does not suffer any additional shift because the susceptibility is very low even at the resonance. Including the effects of the eddy currents and of the finite demagnetization factor  $D = 0.08$ , we obtain  $f_s = 74 \pm 6 \text{ Hz}$  and  $R = -0.9 \pm 0.1$ . Pure dipolar interaction in rhodium would give  $f_s = 54 \text{ Hz}$ , and the remaining shift is attributed to the pseudodipolar exchange term  $f_{pd} = 20 \pm 6 \text{ Hz}$  [17]. If the isotropic exchange is compared with the actual dipolar interaction alone, i.e.,  $R = \sum_j J_{ij} I^2/\mu_0 \mu^2 \rho$ , we would have  $R = -1.2$ , which is close to the value adopted by Hakonen *et al.* [18]. Neither of the comparisons is entirely meaningful without knowing the true range function of the pseudodipolar term. This would require detailed information about the conduction electron band of rhodium [16]. The simplest approach is to use an effective moment  $\mu_{\text{eff}} = \sqrt{Ihf_s/\mu_0 \rho} = 0.10\mu_N$ . This is evidently too crude a simplification because the anisotropic nearest neighbor contribution is then underestimated due to the oscillatory nature of the indirect interactions.

Further analysis of the data deals with the relative intensity  $I_r = I_2/I_1$  of the two peaks. In terms of the coupling constant  $A$ ,  $I_r$  may be expressed as [6,7]

$$\begin{aligned} I_r &= A/(f_- - f_2)^2 \\ &= 4A/(f_2 - f_1 + \sqrt{(f_2 - f_1)^2 + 4A})^2 \\ &= 4A'/(B_1 - B_2 + \sqrt{(B_1 - B_2)^2 + 4A'})^2, \end{aligned} \quad (4)$$

where the last form with  $A' = A(Ih/2\mu)^2$  is relevant for field-sweep measurements at a constant excitation frequency. The polarization dependence of the expression lies in  $B_1 - B_2$ , reducing the data so that it falls on a universal curve.

The quantitative intensity analysis is troublesome because of the weakness of the double-spin-flip resonance in close vicinity to the main peak, so that the baseline for the second harmonic is not very well established. This is evident by looking at the inset of Fig. 2. A Gaussian

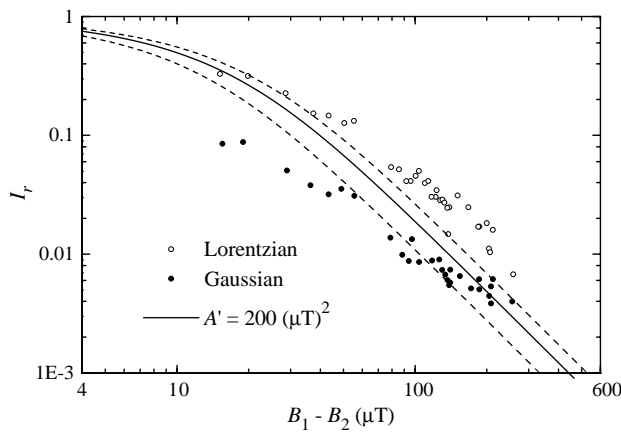


FIG. 4. Relative intensity of the double-spin-flip mode and the Larmor mode as a function of the separation of the two peaks. The solid line represents Eq. (4) with  $A = 1400 \text{ Hz}^2$  ( $A' = 200 \mu\text{T}^2$ ). The dashed lines correspond to the limits given in the text. The two data sets are obtained by using Lorentzian or Gaussian fits for the double-spin-flip peak.

fit for the satellite peak produces as good a result as a Lorentzian fit, but the total areas obtained can differ by as much as a factor of 4 because of the adjusted baseline level. Judging on the basis of the parallel-field data, the second harmonic is Gaussian at least when it is well separated from the main line. On the other hand, at the crossing point the two resonances have equal intensities [see Eq. (4)], whereas experimentally we observe a single inseparable broadened Lorentzian line. This suggests that the line shape of the second harmonic changes from Gaussian to Lorentzian when approaching the line crossing. We were unable to follow such a gradual change by just looking at the resonance shapes, but the fitted intensities do agree better with Eq. (4), if such an assumption is made.

The intensity ratios are plotted in Fig. 4, where both Gaussian and Lorentzian fits are displayed. The data can be represented by a theoretical curve of Eq. (4) by using a compromise value of  $A = 1400 \pm 600 \text{ Hz}^2$ . This number is reasonable and can be compared with that computed for silver,  $A_{\text{Ag}} \sim 1 \times 10^3 \text{ Hz}^2$  [7], whose relevant parameters are quite similar. For materials with identical lattice structures  $A$  scales as  $\mu^4 \rho^2 (I + 1) / I^3$  [7]. If the value for copper,  $A_{\text{Cu}} \sim 1 \times 10^7 \text{ Hz}^2$  [6], is used as a reference, our result is about 4 times larger than expected. This could result from the enhancement of the nearest neighbor coupling due to the pseudodipolar term. The above value for  $A$  was used to implement Fig. 3 with the coupled mode frequencies  $f_+$  and  $f_-$  of Eq. (3).

In conclusion, we were able to observe a second-order resonance in the highly polarized nuclear-spin system of rhodium at positive and negative spin temperatures by high sensitivity SQUID-NMR measurements. The observed line shifts and relative intensities yield direct information of the mutual interactions between the spins, which is essential for making predictions upon spontaneous magnetic ordering. Considering the feasibility of making similar measurements on other metals, such as silver or gold, at least the parallel-field absorption should be detectable by our double-excitation method, as in Fig. 1, since then the weak secondary line is not overwhelmed by the strong primary peak.

We acknowledge useful discussions with M. Paalanen and P. Hakonen. This work was supported by the ULTI II grant of the European Union.

\*Permanent address: Dept. Cond. Matt. Phys., Risø National Laboratory, 4000 Roskilde, Denmark.

†Present address: VTT Automation, Measurement Technology, P.O. Box 1304, FIN-02044 VTT, Finland.

‡Present address: Lyman Laboratory, Harvard University, Cambridge, MA 02138.

- [1] A.S. Oja and O.V. Lounasmaa, *Rev. Mod. Phys.* **69**, 1 (1997).
- [2] J.H. Van Vleck, *Phys. Rev.* **74**, 1168 (1948).
- [3] H. Cheng, *Phys. Rev.* **124**, 1359 (1961).
- [4] A.G. Anderson, *Phys. Rev.* **115**, 863 (1959).
- [5] M. Kohl *et al.*, *J. Low Temp. Phys.* **72**, 319 (1988).
- [6] J.P. Ekström *et al.*, *Physica (Amsterdam)* **98B**, 45 (1979).
- [7] P.L. Moyland, P. Kumar, J. Xu, and Y. Takano, *Phys. Rev. B* **48**, 14020 (1993).
- [8] P.J. Hakonen and S. Yin, *J. Low Temp. Phys.* **85**, 25 (1991).
- [9] J.T. Tuoriniemi *et al.*, *Phys. Rev. Lett.* **75**, 3744 (1995).
- [10] W. Yao *et al.* (to be published).
- [11] T.A. Knuuttila *et al.* (to be published).
- [12] P.J. Hakonen, S. Yin, and O.V. Lounasmaa, *Phys. Rev. Lett.* **64**, 2707 (1990).
- [13] R.T. Vuorinen, P.J. Hakonen, W. Yao, and O.V. Lounasmaa, *J. Low Temp. Phys.* **98**, 449 (1995).
- [14] J.A. Osborn, *Phys. Rev.* **67**, 351 (1945).
- [15] A. Abragam, M. Chapellier, J.F. Jacquinet, and M. Goldman, *J. Magn. Reson.* **10**, 322 (1973).
- [16] N. Bloembergen and T.J. Rowland, *Phys. Rev.* **97**, 1679 (1955).
- [17] A. Narath, A.T. Fromhold, Jr., and E.D. Jones, *Phys. Rev.* **144**, 428 (1966).
- [18] P.J. Hakonen, R.T. Vuorinen, and J.E. Martikainen, *Phys. Rev. Lett.* **70**, 2818 (1993).